

# On viscosity, conduction and sound waves in the intracluster medium

A. C. Fabian,<sup>1</sup>\* C. S. Reynolds,<sup>2</sup> G. B. Taylor<sup>3,4</sup> and R. J. H. Dunn<sup>1</sup>

<sup>1</sup>*Institute of Astronomy, Madingley Road, Cambridge CB3 0HA*

<sup>2</sup>*Department of Astronomy, University of Maryland, College Park, MD 20742, USA*

<sup>3</sup>*Kavli Institute of Particle Astrophysics and Cosmology, Menlo Park, CA 94025, USA*

<sup>4</sup>*National Radio Astronomy Observatory, PO Box O, Socorro, NM 87801, USA*

Accepted 2005 August 2. Received 2005 July 12; in original form 2004 December 23

## ABSTRACT

Recent X-ray and optical observations of the Perseus cluster indicate that a combination of weak shocks at small radii ( $\gtrsim 20$  kpc) and viscous and conductive dissipation of sound waves at larger radii is responsible for heating the intracluster medium and can balance radiative cooling of cluster cores. We discuss this mechanism more generally and show how the specific heating and cooling rates vary with temperature and radius. It appears that this heating mechanism is most effective above  $10^7$  K, which allows for radiative cooling to proceed within normal galaxy formation but stifles the growth of very massive galaxies. The scaling of the wavelength of sound waves with cluster temperature and feedback in the system are investigated.

**Key words:** galaxies: clusters: general – cooling flows – X-rays: galaxies.

## 1 INTRODUCTION

The H $\alpha$ -emitting filaments surrounding NGC 1275 in the core of the Perseus cluster (Lynds 1970; Conselice, Gallagher & Wyse 2001) appear to act as streamlines revealing flows in the intracluster medium (ICM) (Fabian et al. 2003b). Many of the outer filaments are reasonably straight and stretch over tens of kiloparsecs. One, dubbed the horseshoe (Conselice et al. 2001), folds back on itself just behind a large spherical-cap-shaped depression in the X-ray intensity of the gas, suggestive of the flow on Earth seen behind rising spherical-cap bubbles in water (Fabian et al. 2003b). Together these observations indicate that the ICM is not highly turbulent and is probably viscous, with a viscosity approaching the Spitzer (1956) value for an ionized plasma.

Further evidence for the medium being viscous is provided by the *shape* of detached buoyant bubbles, seen most clearly in the Perseus cluster (Fabian et al. 2003a). Simulations of bubbles rising in an ICM show that viscosity enables bubbles to remain intact for longer than a crossing time (Reynolds et al. 2005). Strong magnetic fields are otherwise required to prevent bubbles from breaking up.

If the ICM is viscous then sound waves produced, for example, by radio bubbles from the central active galaxy, as seen in the Perseus cluster (Fabian et al. 2003a), can be rapidly dissipated. This provides an efficient mechanism for transferring energy produced by a massive black hole in a central cluster galaxy into the surrounding medium in a reasonably isotropic manner (see also Ruszkowski, Brügggen & Begelman 2004a,b). Although the energy flow passes through highly directional jets, the resultant bubbling produces

approximately spherical sound waves which propagate into the cluster.

Energetic outflows from black holes do not otherwise couple well to surrounding gas. Electromagnetic ones pass through the gas which, being ionized, is mostly transparent. Collimated outflows, which tend to be the most energetic, are often too violent and bore right through the gas along the collimation direction (e.g. Cygnus A; Hydra A, McNamara et al. 2005). Uncollimated winds might work but would tend to give strong shocks, which are not observed in the inner intracluster gas. Viscous dissipation can provide continuous, gentle, distributed heat (Fabian et al. 2003a), as is required (Voigt & Fabian 2004).

Here, we examine the dissipation of sound wave energy in intracluster and intragroup gas due to both viscosity and thermal conduction. Both of these transport processes have a strong temperature dependence which means that such heating dominates over radiative cooling above about  $10^7$  K. Radiative cooling dominates below that temperature. This provides a clue as to why heating appears to stifle the cooling in clusters and groups (the cooling flow problem: see Fabian et al. 2001) yet most galaxy formation, where much of the stellar component is a consequence of radiative cooling of baryons which have fallen into dark matter wells, has taken place. Indeed, the process that stifles cooling in massive systems probably is responsible for truncating the upper mass range of galaxies (Fabian, Voigt & Morris 2002; Benson et al. 2003; Binney 2004).

## 2 VISCOUS AND CONDUCTIVE HEATING

### 2.1 Sound wave heating and radiative cooling rates

We now consider the ICM heating rate caused by the dissipation of radio galaxy induced sound waves. Suppose that the ICM possesses

\*E-mail: acf@ast.cam.ac.uk

a kinematic viscosity  $\nu$  and a thermal conductivity  $\kappa$ . The absorption coefficient for the passage of sound waves is given by (Landau & Lifshitz 1987)

$$\gamma = \frac{2\pi^2 f^2}{c_s^3} \left[ \frac{4}{3}\nu + \frac{\kappa}{\rho} \left( \frac{1}{c_v} - \frac{1}{c_p} \right) \right], \quad (1)$$

where  $f$  is the frequency of the sound waves,  $c_s$  is the sound speed,  $\rho$  is the density of the ICM, and  $c_v$  and  $c_p$  are the specific heats at constant volume and pressure, respectively. The dissipation length (i.e. the length-scale over which the energy flux of the sound wave decreases by a factor of  $e$ ) is given by  $\ell = 1/2\gamma$ . Noting that  $c_p/c_v = 5/3$  for a fully ionized gas, we can write

$$\ell = \frac{3c_s^3}{8\pi^2 f^2 (2\nu + \kappa/\rho c_p)}. \quad (2)$$

We note that this expression is only strictly true in the regime in which the wavelength of the sound waves is short compared with the dissipation length  $\ell$ . We briefly discuss a possible violation of this condition later in this section. Now, suppose that the viscosity and thermal conductivity are fixed fractions,  $\xi_\nu$  and  $\xi_\kappa$ , of their unmagnetized values. For a fully ionized hydrogen plasma, in c.g.s. units, we get

$$\nu = 1.0 \times 10^{25} T_7^{5/2} n^{-1} \xi_\nu, \quad (3)$$

$$\frac{\kappa}{\rho c_p} = 2.36 \times 10^{26} T_7^{5/2} n^{-1} \xi_\kappa, \quad (4)$$

where  $T_7 = T/(10^7 \text{ K})$ , and  $n$  is the electron number density, and we have taken the Coulomb logarithm to have a value of 37. Substituting the numerical values into equation (2), we get

$$\ell = 697 \frac{n T_7^{-1} f_{-6}^{-2}}{(\xi_\nu/0.1) + 11.8(\xi_\kappa/0.1)} \text{ kpc}, \quad (5)$$

where we have expressed the sound wave frequency in units of per megayear (i.e.  $f_{-6} = f/(10^{-6} \text{ yr}^{-1})$ ) and have normalized to plausible values of viscosity and thermal conductivity (following the arguments of Narayan & Medvedev 2001). Hereafter, we shall denote

$$\bar{\xi} = \frac{\xi_\nu}{0.1} + 11.8 \frac{\xi_\kappa}{0.1}. \quad (6)$$

We note that, since temperature and density vary with radius in the cluster, the dissipative effects of viscosity and thermal conductivity vary but maintain a fixed ratio (as a consequence of assuming that  $\xi_\nu$  and  $\xi_\kappa$  are constant). We also note that thermal conduction is over an order of magnitude more effective at dissipating sound wave energy if  $\xi_\nu \approx \xi_\kappa$ .

We now model the central active galactic nucleus (AGN) as a source of acoustic energy at the centre of the cluster. Suppose that the AGN injects an acoustic luminosity of  $L_{\text{inj}}$  into the ICM at an inner radius of  $r = r_{\text{in}}$ . If  $L_s(r)$  is the acoustic luminosity at radius  $r > r_{\text{in}}$ , the definition of dissipation length gives

$$\frac{dL_s}{dr} = -\frac{L_s}{\ell}, \quad (7)$$

which has the solution

$$L_s(r) = L_{\text{inj}} \exp\left(-\int_{r_{\text{in}}}^r \frac{1}{\ell} dr\right). \quad (8)$$

The volume heating rate due to viscous and conductive dissipation is

$$\epsilon_{\text{diss}} = \frac{L_s(r)}{4\pi r^2 \ell}, \quad (9)$$

which for  $r \ll \ell$  is approximately

$$\epsilon_{\text{diss}} \approx \frac{2\pi f^2 L_{\text{inj}} (2\nu + \kappa/\rho c_p)}{3c_s^3 r^2}, \quad (10)$$

and can be evaluated to give

$$\epsilon_{\text{diss}} \approx 3.8 \times 10^{-29} T_7 n^{-1} f_{-6}^2 r_2^{-2} L_{44} \bar{\xi} \text{ erg cm}^{-3} \text{ s}^{-1}, \quad (11)$$

where  $L_{44} = L_{\text{inj}}/(10^{44} \text{ erg s}^{-1})$  and  $r_2 = r/(100 \text{ kpc})$ .

As illustrations of the radial dependence of the viscous and conductive dissipation, we compute  $\epsilon_{\text{diss}}$  using the temperature and density profiles of Abell 2199 from Johnstone et al. (2002;  $T = 4.4 r_2^{0.3} \text{ keV}$  and  $n = 6.0 \times 10^{-3} r_2^{-0.75} \text{ cm}^{-3}$ ) and beyond about 20 kpc in the core of the Perseus cluster from Sanders et al. (2004;  $T = 5.84 r_2^{0.44} \text{ keV}$  and  $n = 1.0 \times 10^{-2} r_2^{-1.1} \text{ cm}^{-3}$ ). We compare these with the radiative cooling as derived from the formula of Tozzi & Norman (2001) which, expressed in our units, becomes

$$\epsilon_{\text{rad}} = 10^{-24} n_i n_e (1.13 T_7^{-1.7} + 5.3 T_7^{0.5} + 6.3). \quad (12)$$

As shown in Fig. 1, the dissipative heating can be comparable to or exceed the radiative cooling within the fiducial cooling radius in which the cooling time  $\tau = 3nkT/2\epsilon_{\text{rad}}$  exceeds 3 Gyr. Indeed, in the case of Abell 2199, the dissipative heating closely balances the radiative cooling out to the cooling radius for the following choice of parameters:  $L_{44} = 1$ ,  $f = 0.2$ ,  $\xi_\nu = 0.1$ ,  $\xi_\kappa = 0$ . The dissipation length-scale is approximately 100 kpc, and the heating rate displays a power-law radial profile within this radius (reflecting the simple power-law forms of the assumed temperature and density). A sharp (exponential) cut-off in the heating rate is seen for radii larger than the dissipation length. Varying the acoustic luminosity of the AGN simply changes the normalization of this heating rate. On the other hand, varying the frequency of the sound waves leads to dramatic changes in the dissipation length-scale. In particular, increasing the sound frequency while leaving the other parameters at the values listed above rapidly brings the dissipation length-scale within the cooling radius. A detailed balance of heating and cooling is then no longer possible – the innermost regions can be strongly heated while radiative cooling occurs unchecked at the cooling radius. In the case of the Perseus cluster, the steep density profile results in the radiative cooling possessing a significantly stronger radial dependence than the ‘monochromatic’ (i.e. single frequency) dissipative heating profile. Thus any balance between sound wave dissipation and radiative cooling must employ acoustic waves with a range of frequencies.

To quantify this, suppose that the injected acoustic luminosity between frequencies  $f$  and  $f + df$  is  $L_{\text{inj}}(f) df$ . Furthermore, suppose that all frequencies are injected at the same radius  $r = r_{\text{in}}$ . The full expression for the dissipative heating is then

$$\epsilon_{\text{diss}} = \int_0^\infty \frac{L_{\text{inj}}(f)}{4\pi r^2 \ell} \exp\left(-\int_{r_{\text{in}}}^r \frac{1}{\ell} dr\right) df. \quad (13)$$

For comparison with Perseus, it is useful to quantify the flattening of the dissipation profile due to the spectrum of frequencies in the case of power-law radial dependences of temperature and density. Suppose that  $T \propto r^\alpha$  and  $n \propto r^{-\beta}$ , where we expect  $\alpha, \beta > 0$  on general physical grounds. Using equation (11) we can then approximate the dissipative heating profile of a given frequency as a power law in radius,

$$\epsilon_{\text{diss}}(f) \propto r^{\alpha+\beta-2} f^2 L_{\text{inj}}(f), \quad (14)$$

which is truncated at radius  $r = \ell$ . Suppose that the spectrum of frequencies has a power-law form,  $L_{\text{inj}}(f) \propto f^{-\gamma}$  between  $f = f_{\text{min}}$  and  $f = f_{\text{max}}$ . Noting that  $\ell$  increases with decreasing frequency, we can delineate the following regimes.

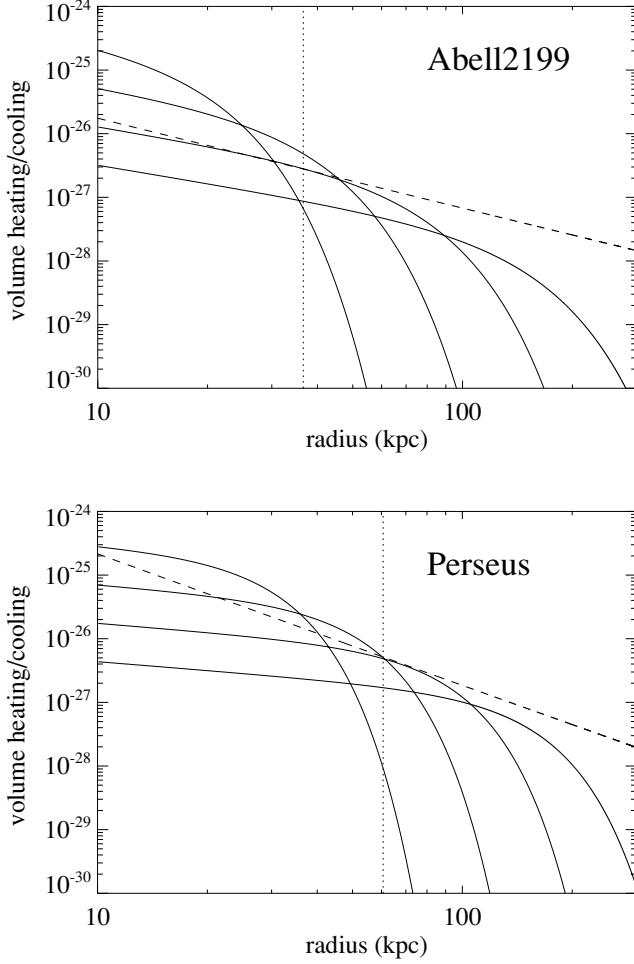


**Figure 1.** Dissipative volume heating rates (solid lines) and radiative volume cooling rate (dashed line), using the temperature and density profile of (top) Abell 2199 (Johnstone et al. 2002) and (bottom) the core of the Perseus cluster (Sanders et al. 2004). The lowest solid line is for the following illustrative set of parameters for which the heating and cooling approximately balance:  $L_{44} = 1$  for Abell 2199, 5 for Perseus,  $f_{-6} = 0.1$ ,  $\xi_v = 0.1$ ,  $\xi_\kappa = 0$ . Other choices of the acoustic power ( $L_{44}$ ) will simply rescale this line in the vertical direction. Other choices of  $f_{-6}$ ,  $\xi_v = 0.1$  and  $\xi_\kappa = 0$  change the dissipation length-scale as well – the family of additional (thin) solid lines shows the effect of successive doublings of frequency ( $f_{-6} = 0.2, 0.4$  and  $0.8$ ). The vertical dotted lines indicate a fiducial cooling radius where the radiative cooling time of the gas is 3 Gyr.

(i) If  $r > \ell(f_{\min})$ , the radius under consideration is outside the overall dissipation region and the dissipative heating profile is rapidly declining.

(ii) If  $r < \ell(f_{\max})$ , even the highest frequency component has not yet dissipated away and the radial dependence of the heating is just the sum of similar monochromatic components,  $\epsilon_{\text{diss}} \propto r^{\alpha+\beta-2}$ .

(iii) If  $\ell(f_{\max}) < r < \ell(f_{\min})$ , only the frequency components up to  $f = \tilde{f}$  contribute, where  $\tilde{f}$  is defined by  $r = \ell(\tilde{f})$ . In this case,

$$\epsilon_{\text{diss}} \propto \int_{f_{\min}}^{\tilde{f}} r^{\alpha+\beta-2} f^{2-\gamma} df. \quad (15)$$

For  $\gamma > 3$ , the lowest frequencies always dominate the energetics and we again get the monochromatic case  $\epsilon_{\text{diss}} \propto r^{\alpha+\beta-2}$ . For  $\gamma < 3$ ,

we get  $\epsilon_{\text{diss}} \propto r^\delta$ , where

$$\delta = \alpha + \beta - 2 - \frac{(3 - \gamma)(\alpha + \beta + 1)}{2}. \quad (16)$$

The second term on the right-hand side of the last expression represents the modification of the monochromatic result due to the spectrum of frequencies.

Using these results, we can predict that for dissipative heating to balance radiative cooling in the Perseus cluster, we require a spectrum of fluctuations with  $\gamma \approx 1.8$  across at least the frequency range  $f_{-6} = 0.2-1$ .

For a given suppression factor ( $\xi_v$  and  $\xi_\kappa$ ), thermal conduction can be significantly more important than viscosity at dissipating sound wave energy. However, this is only strictly true when the dissipation wavelength is large compared with the wavelength of sound. If the thermal conduction is such that the dissipation length-scale  $\ell$  is comparable to or smaller than the wavelength of the sound wave under consideration, dissipation due to thermal conduction will be *ineffective* and the sound wave will propagate as an isothermal sound wave. Indeed, if thermal conduction occurred at the level suggested by Narayan & Medvedev (2001),

$$\xi_\kappa \approx 0.2, \quad (17)$$

the dissipation length-scale would be extremely short for all but the lowest frequency sound waves ( $\ell \approx 150 f_{-6}^{-2}$  pc using  $n = 0.02 \text{ cm}^{-3}$  and  $T_7 = 4$ ). Thus an implicit prediction of Narayan & Medvedev (2001) is that the sound waves observed in the Perseus cluster are isothermal sound waves. Indeed, the thermal conduction can become so ineffective at dissipating acoustic energy that viscous dissipation dominates even if  $\xi_\kappa > \xi_v$ .

The theory outlined above only strictly applies to the case of linear sound waves; this imposes a radius-dependent maximum acoustic luminosity to which this theory can be applied. Expressed in terms of pressure fluctuations,  $\delta p$ , the acoustic luminosity crossing a shell at radius  $r$  is

$$L_s \approx 4\pi r^2 \frac{\delta p^2}{\rho c_s}. \quad (18)$$

The acoustic waves become strongly non-linear when  $\delta p \approx p$ . Thus the maximum acoustic luminosity for which our model applies is

$$L_{s,\text{max}} \approx 4\pi r^2 \frac{p^2}{\rho c_s} \approx 3.1 \times 10^{46} n T_7^{1.5} r_2^2 \text{ erg s}^{-1}. \quad (19)$$

Using this equation, we see that the fiducial model described above for Abell 2199 ( $L_{44} = 1$ ,  $f = 0.1$ ,  $\xi_v = 0.1$ ,  $\xi_\kappa = 0$ ) is only valid for radii greater than about 20 kpc. Within that radius, the energy must be transported within the form of shocks and/or strong convective motions.

For comparison, we now consider the dissipation rate in a weak shock,  $\epsilon_{\text{shock}} \propto (\delta P/P)^3 p f$  (Stein & Schwartz 1972; Landau & Lifshitz 1987):

$$\epsilon_{\text{shock}} \approx 4 \times 10^{-28} L_{44}^{3/2} n^{-1/2} T_7^{-5/4} r_2^{-3} f_{-6} \text{ erg cm}^{-3} \text{ s}^{-1}. \quad (20)$$

This is comparable to the required heating rate at about 10–20 kpc radius in the Perseus cluster (where a weak shock is seen: Fabian et al. 2003a) if  $f_6 \sim 0.1$  and  $L_{44} \sim 10$ . For the density and temperature profiles of that cluster,  $\epsilon_{\text{diss}} \propto r^{-0.46}$  and  $\epsilon_{\text{shock}} \propto r^{-3}$ . Viscous dissipation is therefore most effective at larger radii and for higher frequencies, shock dissipation applying most to small radii and low frequencies. Since 96 per cent of the *volume* within 60 kpc lies beyond 20 kpc, it is reasonable to state that viscous heating can dominate the volume heating.

## 2.2 A note on the effect of magnetic fields in the ICM

In the above analysis, the viscosity and thermal conductivity were assumed to be a fixed fraction of the Spitzer (1956) value for an ionized gas. Cluster cores do have significant magnetic fields (e.g. Carilli & Taylor 2002) which may of course alter the viscosity. What effect this has is unclear.

There is, however, evidence from Faraday rotation measure (RM) observations (Carilli & Taylor 2002, and references therein) that the field is coherent in patches larger than the ion mean free path. Typical values of the cell size estimated from RM distributions and quoted in the literature are 5–10 kpc. A power spectrum analysis of Hydra A, a bright radio galaxy and one of the best cases for probing a cooling core cluster as it provides a probe of the RM distribution on scales from 0.2 to 40 kpc, has been carried out by Vogt & Ensslin (2005), who find a magnetic autocorrelation length of  $3 \pm 0.5$  kpc. This autocorrelation length can be compared to the ion mean free path (mfp) of  $0.23 T_c^2 n_c^{-1}$  kpc for typical cluster core parameters of  $T_c = 3 \times 10^7$  K and  $n_c^{-1} = 0.01 \text{ cm}^{-3}$ . Since the mfp is smaller than the dominant scale-size of the magnetic field, the viscosity along the magnetic field direction will be high for much of the volume under consideration. This is also relevant to the issue of conduction, which can also dissipate the energy in sound waves (Landau & Lifshitz 1987; see also Ruszkowski, Brüggén & Hallman 2005), but is not strong enough to offset cooling in many clusters by itself (Voigt & Fabian 2004; Kaastra et al. 2004).

The simple model considered in Section 2.1 can be motivated from the notion that ICM consists of many magnetically isolated blobs of gas, each of size ranging over a few kpc. Within a blob the field is fairly coherent. Conduction of heat from the outside of the core to the centre is inhibited by the boundaries between the blobs. The energy in sound waves propagates freely across the blob boundaries and can be dissipated within the blobs by both conduction and viscosity.

There are other possible sources of viscosity in a tangled magnetic field. For example, if the field is in the form of flux tubes there can be drag between the high-field regions and the low-field ones (Longcope, McLeish & Fisher 2003). Alternatively, the spatial configuration of the field may change as sound waves pass across a region in the sense that shaking up the field causes it to shift to a lower energy configuration, so releasing energy either immediately or later. This would operate as a bulk viscosity. [The issue of bulk viscosity is also mentioned by Ruszkowski et al. (2004a).]

## 3 THE WAVELENGTH AND FREQUENCY OF SOUND WAVES

Subcluster mergers are common in clusters, and these will generate large pressure discontinuities and sound waves. The wavelengths of sound waves remaining after shocks have passed will presumably be on the scale of cluster cores or hundreds of kiloparsecs. On these scales the gas may be turbulent so the motions may degrade down to scales of tens of kiloparsecs where viscous dissipation can operate. The outer gas in a cluster may therefore be noisy with a wide spectrum of wavelengths. Pringle (1989) noted that the dense regions of a cluster core can focus sound waves inward, meaning that significant heating may result at the centre. Fujita, Matsumoto & Wada (2004), using a 2D simulation, claim that such motions generate strong turbulence. Establishing the energetics and efficiency of such processes requires numerical calculations beyond the scope of this paper. We note that propagating turbulence inward, where the

gravitational potential is steep and the gas dense, is energetically challenging.

A central active nucleus giving rise to jets will inflate cavities of relativistic radio-emitting plasma within the ICM. Such cavities or bubbles are seen in the Perseus cluster (Böhringer et al. 1993; Fabian et al. 2000, 2003a), the Virgo cluster (Wilson & Yang 2002; Forman et al. 2003), A2052 (Blanton et al. 2001; Blanton, Sarazin & McNamara 2003), A2597 (Nulsen et al. 2002), A4059 (Heinz et al. 2002) and Hydra A (McNamara et al. 2000). Such bubbles inflate and then break away as a result of buoyancy (Churazov et al. 2000, 2001) and so even a constant jet will lead to a bubbling effect. This generates a repetitive pressure excess and thus a sound wave with a period equal to the repetition time of the bubbles.

A bubble expands because of its excess pressure relative to the ICM at a rate which varies as  $t^{1/3}$ , where  $t$  is time. It detaches from the jet when buoyancy dominates which is roughly when its expansion velocity drops to about one-half of the local Keplerian velocity due to the local gravitational field of the central galaxy and cluster,  $v_K$  (Churazov et al. 2000). A new bubble then begins to grow. This gives a natural bubbling period  $f \propto L^{-1/2} P^{1/2} v_K^{3/2}$ , where  $P$  is the pressure of the intracluster gas and  $L$  is the power of the jet. Now the central cooling time of many clusters with cool cores levels off at about  $10^8$  yr within a radius of 10 kpc (Voigt & Fabian 2004), which implies that (between clusters)  $P \propto T^{3/2}$ . If we also assume that  $v_K \propto T^{1/2}$  where the gas temperature is  $T$ , then  $f \propto L^{-1/2} T^{3/2}$  and further scaling depends on  $L$ .

The dependence of  $L$  on  $T$  is probably fairly steep. If we assume that the jet power  $L$  does balance cooling then it is proportional to the X-ray luminosity  $L_{\text{cool}}$ , within the cooling radius (where the cooling time equals the cluster age).  $L_{\text{cool}}$  is tabulated for nearby clusters by Peres et al. (1998), and using these values and the cluster temperatures we find (Fig. 2) that  $L \propto T^\alpha$  with  $\alpha \sim 4$ . Therefore  $f \propto T^{-1/2}$ . As a rough check, the scaling predicts that the radius  $R$  when a bubble separates  $R \propto L^{1/2} P^{-1/2} v_K^{-1/2} \propto T$ . This scaling result is shown in Fig. 3 with results for individual clusters drawn from the compilation of Dunn & Fabian (2004).

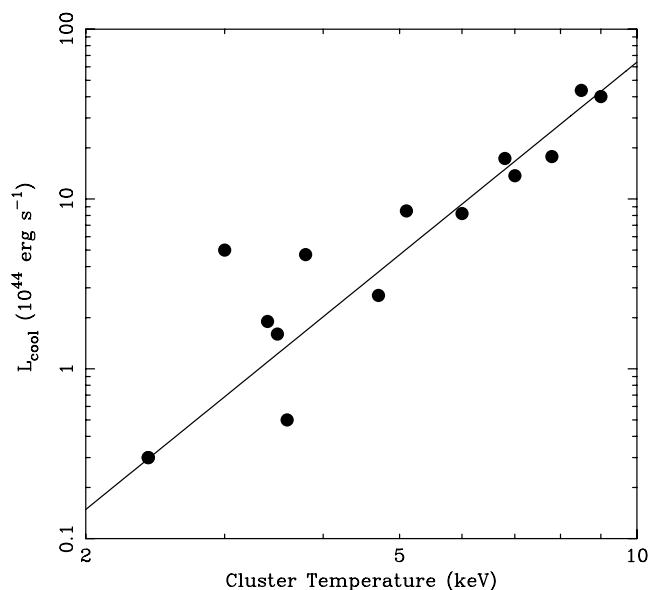


**Figure 2.** The X-ray luminosity within the cooling radius plotted against the cluster temperature, using results for cooling flow clusters taken from Peres et al. (1998). The best-fitting power law is shown, with index 3.8.

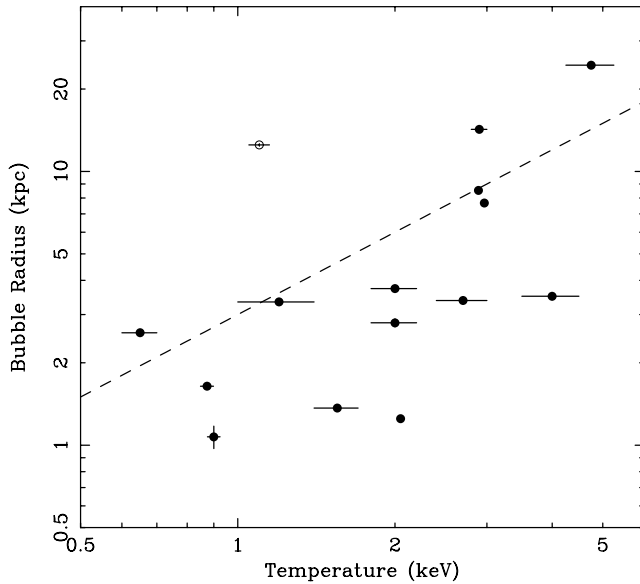


**Figure 3.** The radius of bubbles is shown as a function of the surrounding temperature. Data are for attached bubbles from the compilation of Dunn & Fabian (2004). The open point is for A2052 where there appears to be much cool gas accumulated around the rims (Blanton et al. 2003) so the points may reasonably shift to the right. The dashed line is not a fit but indicates the  $R \propto T$  relation tentatively derived in the text for the rough radius,  $R$ , at which bubbles detach from the nucleus. Bubbles should therefore only exist below, or close to, the line.

The luminosity drops out of the dissipation formula (11) which now varies steeply with temperature:  $\epsilon_{\text{diss}} \propto T^{7/2} r^{-2}$  and at a given radius  $\epsilon_{\text{diss}}/\epsilon_{\text{rad}} \propto T^2$ .

Although we have in this section identified the bubbling frequency as the dominant one, we speculate that the underlying variability of the radio jets occurs at higher frequencies and carries much power. Most jets are not constant, as shown by repeated outbursts on small scales (e.g. in Perseus A = 3C 84: Taylor & Vermeulen 1996; see also Reynolds & Begelman 1997, and in general Zensus 1997). These variations will be transmitted through to the surface of the bubble, leading to its growth being erratic and a spectrum of high-frequency sound waves being present at small radii, with the bubbling frequency being the low-frequency cut-off. The steep dependence on frequency means that higher frequency waves are damped most easily. A simple estimate of the heating effect of bubbles from the bubble size and recurrence rate (e.g. Birzan et al. 2004) will underestimate the true heating rate.

As an indication of the temperature dependence of the dissipation versus radiative cooling, we show  $\epsilon_{\text{diss}}$  and  $\epsilon_{\text{rad}}$  as functions of temperature in Fig. 4. We assume that  $f_{-6}^2 L_{44} \bar{\xi} = 1$ ,  $r = 10$  kpc and  $P = nT = 10^6 \text{ cm}^{-3} \text{ K}$ , which means that if the above scaling is correct, the heating rate in real objects is steeper. The plot shows that sound wave dissipative heating dominates above about  $10^7$  K and radiation dominates below. The process is therefore relevant as an explanation for the truncation of cooling, and thus of star formation and the total stellar mass, in massive galaxies.

#### 4 DISCUSSION

We have shown that viscous heating of intracluster or intragroup gas can effectively compete with radiative cooling above gas temperatures of about  $10^7$  K. The repetitive  $P dV$  work done by the

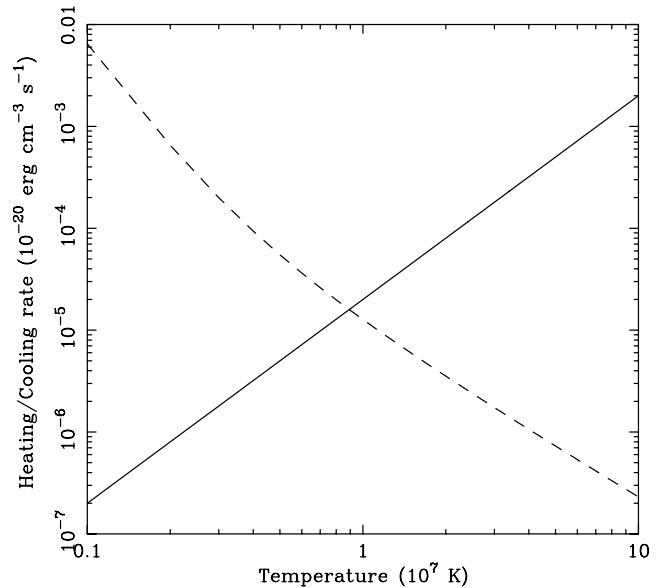


**Figure 4.** Heating (solid) and cooling (dashed) rates plotted as a function of temperature for a pressure  $nT = 10^6 \text{ cm}^{-3} \text{ K}$  and a radius of 10 kpc. For the heating rate,  $f_{-6}^2 L_{44} \bar{\xi} = 1$ .

formation of bubbles is dissipated by weak inner shocks and outer viscous processes. More rapid intrinsic variability in the jets leads to quasi-continuous generation of higher frequency sound waves which dissipate throughout the cooling region. Sound waves produced by jets from a central black hole can thereby strongly reduce cooling in the surrounding gas and prevent further growth of the central galaxy by accretion of radiatively cooled gas. This mechanism may explain the upper mass cut-off in galaxies since it operates best at high temperatures.

If cooling initially dominated in a cluster core then the temperature profile would have dropped to the *local* virial one, which for a NFW potential (Navarro, Frenk & White 1997) approaches  $T \propto r^{1/2}$  for the central cusp (i.e. within the central 100 kpc). Steady heating then applied to this gas will tend to push the gas outward, lowering its density, whereas continued cooling means that gas flows inward, in both circumstances following close to the local virial temperature profile. This roughly explains the observed temperature profiles, given that much of the inner few kiloparsecs are occupied by bubbles.

The prevalence of the central X-ray surface brightness peak characteristic of short radiative cooling times (Peres et al. 1998; Bauer et al. 2005) and the remarkable similarity of the cooling time profiles in many clusters (Voigt & Fabian 2004) suggest that a good heating/cooling balance is commonly established. This presumably requires feedback with the central power source, the accreting black hole. How that is established so that the properties of the gas at, say, 50 kpc are attuned to those at the black hole accretion radius of, say, 100 pc is not completely clear.

A partial answer can be seen from the following. If the radio source becomes too vigorous, then most of its power will be deposited at large radii beyond the cooling radius both if it becomes a Fanaroff–Riley type II (FRII) (as in Cygnus A) or if it remains an FRI when the associated giant bubbles [as in Hydra A (Nulsen et al. 2005) or MS 0735.6 + 7421 (McNamara et al. 2005)] create low-frequency global disturbances which dissipate poorly. If the radio source shuts off as a result of lack of fuel, then the inner gas

will cool and, angular momentum permitting, accrete and provide that fuel. Rapid variations in jet power will lead to high-frequency disturbances which dissipate and so rapidly heat those inner regions. A trickle of cooling and accretion explains the prevalence of warm optical nebulosity (Crawford et al. 1999, and references therein) and cold gas (Edge 1991) near the centres of these objects. The inner cooling time of these objects at  $\sim 10^8$  yr (Voigt & Fabian 2004) is similar to the dynamical time-scale of the central galaxy.

Continued heating by a central AGN in cluster and group cores means that the central black hole continues to grow. The total accreted mass can be considerable (see Fabian et al. 2002; Fujita & Reiprich 2004). This may skew the mass–velocity dispersion relation ( $M-\sigma$ ) for massive black holes upward at the highest black hole masses, such as is expected of the massive black holes in groups and clusters.

Finally, we note that a viscous ICM means that motions in the cores of relaxed clusters will be damped and, apart from the regions directly around the inflating and rising bubbles, or where the dark matter potential or galaxy is sloshing around, fluid motions should be small and highly subsonic ( $\lesssim 0.3 c_s$ ). Of relevance here is the overall scale of any turbulent energy cascade, i.e. the difference in length-scale between the energy injection scale, presumably the bubble size, and the dissipation scale, which may be as large as the size of magnetic cells or similar distinct structures or extend down to much smaller scales. Measurements of the widths and shape of iron K emission lines with a microcalorimeter will help to distinguish laminar motions from turbulence [see Inogamov & Sunyaev (2003) for predictions of turbulent profiles].

## ACKNOWLEDGMENTS

We thank a referee for comments on shock dissipation. CSR gratefully acknowledges support from the *Chandra* Cycle-5 Theory & Modelling programme under grant TM4-5007X. ACF thanks the Royal Society for support.

## REFERENCES

- Bauer F. E., Fabian A. C., Sanders J. S., Allen S. W., Johnstone R. M., 2005, *MNRAS*, 359, 1481
- Benson A. J., Bower R. G., Frenk C. S., Lacey C. G., Baugh C. M., Cole S., 2003, *ApJ*, 599, 38
- Binney J., 2004, *MNRAS*, 347, 1093
- Birzan L., McNamara B. M., Rafferty D. A., Wise M. W., Nulsen P. E. J., 2004, *ApJ*, 607, 800
- Blanton E. L., Sarazin C. L., McNamara B. R., Wise M. W., 2001, *ApJ*, 558, L15
- Blanton E. L., Sarazin C. L., McNamara B. R., 2003, *ApJ*, 585, 227
- Böhringer H., Voges W., Fabian A. C., Edge A. C., Neumann D. M., 1993, *MNRAS*, 264, 25
- Braginskii S. L., 1958, *Sov. Phys. JETP*, 6, 358
- Carilli C. L., Taylor G. B., 2002, *ARA&A*, 40, 319
- Churazov E., Forman W., Jones C., Böhringer H., 2000, *A&A*, 356, 788
- Churazov E., Brügggen M., Kaiser C. R., Böhringer H., Forman W., 2001, *ApJ*, 554, 261
- Conselice C. J., Gallagher J. S., Wyse R. F. G., 2001, *AJ*, 122, 2281
- Crawford C. S., Allen S. W., Ebeling H., Edge A. C., Fabian A. C., 1999, *MNRAS*, 306, 857
- Dunn R. J. H., Fabian A. C., 2004, *MNRAS*, 355, 862
- Edge A. C., 1991, *MNRAS*, 250, 103
- Fabian A. C. et al., 2000, *MNRAS* 318, L65
- Fabian A. C., Mushotzky R. F., Nulsen P. E. J., Peterson J. R., 2001, *MNRAS*, 321, 20
- Fabian A. C., Voigt L. M., Morris R. G., 2002, *MNRAS*, 335, 71
- Fabian A. C., Sanders J. S., Allen S. W., Crawford C. S., Iwasawa K., Johnstone R. M., Schmidt R. W., Taylor G. B., 2003a, *MNRAS*, 344, L43
- Fabian A. C., Sanders J. S., Crawford C. S., Conselice C. J., Gallagher J. S., Wyse R. F. G., 2003b, *MNRAS*, 344, L48
- Forman W. et al., 2003, *astro-ph/0312576*
- Fujita Y., Reiprich T. H., 2004, *ApJ*, 612, 797
- Fujita Y., Matsumoto T., Wada K., 2004, *ApJ*, 612, L9
- Heinz S., Choi Y., Reynolds C. S., Begelman M. C., 2002, *ApJ*, 569, 79
- Inogamov N. A., Sunyaev R. A., 2003, *Astron. Lett.*, 29, 791
- Johnstone R. M., Allen S. W., Fabian A. C., Sanders J. S., 2002, *MNRAS*, 336, 299
- Kaastra J. S. et al., 2004, *A&A*, 413, 415
- Landau L. M., Lifshitz E. M., 1987, *Fluid Mechanics*. Pergamon Press, Oxford
- Longcope D. W., McLeish T. C. B., Fisher G. H., 2003, *ApJ*, 599, 661
- Lynds R., 1970, *ApJ*, 159, 151
- McNamara B. R. et al., 2000, *ApJ*, 534, 135
- McNamara B. R., Nulsen P. E. J., Wise M. W., Rafferty D. A., Carilli C., Sarazin C. L., Blanton E. L., 2005, *Nat*, 433, 45
- Narayan R., Medvedev M. V., 2001, *ApJ*, 562, L129
- Navarro J. F., Frenk C. S., White S. D. M., 1997, *ApJ*, 490, 493
- Nulsen P. E. J., David L. P., McNamara B. R., Jones C., Forman W. R., Wise M., 2002, *ApJ*, 568, 163
- Nulsen P. E. J., McNamara B. R., Wise M. W., David L. P., 2005, *ApJ*, 628, 629
- Peres C. B., Fabian A. C., Edge A. C., Allen S. W., Johnstone R. M., White D. A., 1998, *MNRAS*, 298, 416
- Pringle J. E., 1989, *MNRAS*, 239, 479
- Reynolds C. S., Begelman M. C., 1997, *ApJ*, 487, L135
- Reynolds C. S., McKernan B., Fabian A. C., Stone J. M., Vernaleo J. C., 2005, *MNRAS*, 357, 242
- Ruszkowski M., Brügggen M., Begelman M. C., 2004a, *ApJ*, 611, 158
- Ruszkowski M., Brügggen M., Begelman M. C., 2004b, *ApJ*, 615, 675
- Ruszkowski M., Brügggen M., Hallman E., 2005, *astro-ph/0501175*
- Sanders J. S., Fabian A. C., Allen S. W., Schmidt R. W., 2004, *MNRAS*, 349, 952
- Spitzer L., 1956, *Physics of Fully Ionized Gases*, 1st edn. Wiley-Interscience, New York
- Stein R. F., Schwartz R. A., 1972, *ApJ*, 807
- Taylor G. B., Vermeulen R. C., 1996, *ApJ*, 457, L69
- Tozzi P., Norman C., 2001, *ApJ*, 546, 63
- Vogt C., Ensslin T. A., 2005, *A&A*, 434, 67
- Voigt L. M., Fabian A. C., 2004, *MNRAS*, 347, 1130
- Wilson A. S., Yang Y., 2002, *ApJ*, 568, 133
- Zensus J. A., 1997, *ARA&A*, 35, 607

This paper has been typeset from a  $\text{\TeX}/\text{\LaTeX}$  file prepared by the author.